Paper V

Extraction of the SAW attenuation parameter in periodic reflecting gratings

S. Lehtonen, V. P. Plessky,
C. S. Hartmann, and M. M. Salomaa

V

Extraction of the SAW attenuation parameter in periodic reflecting gratings

Saku Lehtonen, Victor P. Plessky, *Senior Member, IEEE*, Clinton S. Hartmann, *Member, IEEE*, and Martti M. Salomaa, *Member, IEEE*

Abstract

In this paper, the extraction of the coupling-of-modes (COM) model attenuation parameter γ in a finite grating is considered. We use test structures comprising identical transmitting and receiving transducers and a grating centered in the acoustic channel along the propagation direction of the surface acoustic wave (SAW). The extraction procedure proposed is based on studying the magnitude of the ratio of the reflection and transmission coefficients of the grating, R/T, obtained through time gating from the S parameter measurements of the test devices. In particular, it is found that the level of the notches of R/T directly depends on the attenuation of SAW in the grating. A simple closed-form expression for the attenuation normalized to the grating length, $\gamma\lambda_0$, depending on the characteristics of |R/T|, is given. The proposed method is applied to the measurement data for selected grating topologies to yield estimates of the attenuation.

I. Introduction

The coupling-of-modes (COM) model [1] is widely used as a preliminary design tool for surface-acoustic wave (SAW) devices. The reliability of the model is strongly dependent on the accuracy of the COM parameters. There are established methods for the extraction of the reflectivity of the grating and the velocity therein [2], but the attenuation remains difficult to address. In our previous work, estimates were obtained through simulations for long and short reflectors [3, 4]. Here, we present a procedure for the extraction of the attenuation parameter in a finite grating. Our technique is based on the analysis of the frequency-dependent scattering parameters of the simulated and/or measured responses of tailored test structures. The level of notches of the ratio of the reflection and transmission coefficients of the grating, |R/T|, is used for determining the normalized attenuation.

S. Lehtonen (e-mail: saku@focus.hut.fi) and M. M. Salomaa (e-mail: Martti.Salomaa@hut.fi) are with the Materials Physics Laboratory, Helsinki University of Technology, P.O. Box 2200, FIN-02015 HUT, Finland.

V. P. Plessky is with GVR Trade SA, Rue du Château 9 C, CH-2022 Bevaix, Switzerland (e-mail: victor.plessky@bluewin.ch).

C. S. Hartmann is with RF SAW Inc., 900 Alpha Drive, Suite 400, Richardson, TX 75081, USA (e-mail: chartmann@rfsaw.com).

Background and methodology for the analysis of the frequency responses of the test structures are discussed in Sec. II. Theoretical derivation leading to an analytic equation for the normalized attenuation parameter is presented in Sec. III, and the results obtained by applying the proposed procedure to experimental data are shown and discussed in Sec. IV.

II. Methods

A schematic of the test structures used in this work is shown in Fig. 1. The test structure framework comprises two interdigital transducers (IDTs) connected to the electric ports 1 and 2, having 15 fundamental-mode electrodes with the periodicity p ($\lambda_0 = 2p$) each and a center-to-center separation of 600 μm. The metallisation is aluminium and the substrate 128° $LiNbO_3$. The grating studied is centered in the acoustic channel defined by the IDTs, thus yielding equivalent lengths of propagation path for the waves reflected from and transmitted through the grating. The grating consists of either short-circuited or floating electrodes. The relative bandwidth of the IDTs at ports 1 and 2, measured as the distance between the first zeros of the transfer function, can be approximated as

$$\mathrm{BW_{IDT}} = \frac{2}{N_{\text{finger pairs}}}. \tag{1}$$

To properly address the characteristics of the grating, the distance between the first zeros of the reflection coefficient should be lower than that given by Eq. (1). See Fig. 2 for an illustration manifesting the IDT response and the magnitude of the ratio of the reflection and transmission coefficients of a grating. In this connection, very short reflectors including only few fingers are not suitable due to their wideband response possibly comparable to or wider than that of the IDTs. Very long reflectors, on the other hand, imply a large number of multiple reflections and, with the exception of the zeros of the reflection response, a vanishing transmission through the grating. A compromise in the number of fingers

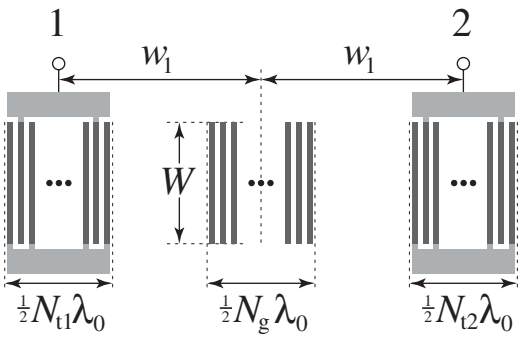

Fig. 1. Schematic of the grating test structure. The distance between the centers of the transmitting and receiving IDTs ($N_{t1} = N_{t2} = 15$) is $2w_1 = 600$ μm and the aperture is $W = 100$ μm. Here, the grating has floating electrodes.

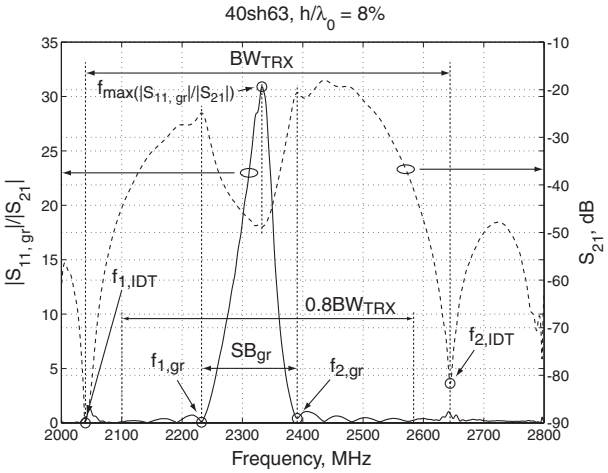

Fig. 2. Response characteristics addressed when extracting the reflectivity of the grating. The solid curve is the ratio of the magnitudes of the reflection and transmission coefficients of a grating ($|R/T| = |S_{11,\,gr}|/|S_{21}|$), where the first notches ($f^1_{1,gr}$ and $f^1_{2,gr}$) around the maximum ($f_{max(|S_{11,\,gr}|/|S_{21}|)}$) define the grating stopband. The first notches of the transducer frequency response of the test structure (dashed curve, $f_{1,IDT}$ and $f_{2,IDT}$) indicate the range of feasibility. Here, the grating within the test structure is short-circuited, has 40 electrodes and the metallisation ratio $a/p = 0.63$. The aluminium thickness $h/\lambda_0 = 8\%$.

combines a rather narrow response with a transmission signal reliably measurable at all frequencies of interest. Here, short-circuited gratings having 20 or 40 electrodes are considered, the metallization ratio and thickness varying within a/p = [0.43, 0.53, 0.63] and h/λ_0 = [5%, 6.5%, 8%], respectively. Due to the higher reflectivity per wavelength of floating electrodes [4], open-circuited gratings having equivalent electrode cross-section profiles but a number of electrodes one half (10 or 20) of that of their short-circuited counterparts are studied. The periodicity of the IDTs and the gratings is 0.8 μm, which yields a center frequency close to 2.5 GHz for the substrate used (128° $LiNbO_3$).

The response of the setup in Fig. 1 is that of a delay line (IDTs) perturbed by a grating. Multiple SAW reflections between the IDTs and the grating manifest themselves as ripples. Using the time gating procedure [5] in a manner described in Refs. [3, 4], the contributions of the pulse reflected once from the grating and registered at port 1 ($S^{\text{time-gated}}_{11,\,gr}$) and the pulse transmitted directly through the grating and registered at port 2 ($S^{\text{time-gated}}_{21}$) can be separated. Their frequency-domain representations within the IDT bandwidth, free of multiple-transit ripples, then illustrate the grating characteristics. A reference signal ($S^{\text{time-gated}}_{21,\,ref}$) can be obtained from a correspondingly time-gated response of a test structure with the grating absent. Comparing the signals carrying information on the grating to the reference, one obtains the frequency-dependent reflection and transmission coefficients of the grating:

$$\begin{aligned} R &= \frac{S^{\text{time-gated}}_{11,\,gr}}{S^{\text{time-gated}}_{21,\,ref}}, \\ T &= \frac{S^{\text{time-gated}}_{21}}{S^{\text{time-gated}}_{21,\,ref}}. \end{aligned} \tag{2}$$

In order to obtain R and T, 2-port data of the device studied and that of the reference device are required. When experimental data is acquired, the possible inaccuracies in the measurements affect the results. However, the need of two separate measurements can be avoided by apprehending that the essential features of the reflection response are reproduced in the ratio of the reflection and transmission responses [6],

$$\frac{R}{T} = \frac{S^{\text{time-gated}}_{11,\,gr}}{S^{\text{time-gated}}_{21}}. \tag{3}$$

In particular, the notches of |R/T| are found at the same frequencies as those of the reflection coefficient |R|. An example of the measured magnitude of the ratio of the reflection and transmission coefficients is shown in Fig. 2. The transmission response of the test structure illustrating the IDT characteristics (main lobe defined by the first notches $f_{1,IDT}$ and $f_{2,IDT}$) is also shown.

Note that in our geometry in Fig. 1, due to the equal distances from the grating to the IDTs, not only the contributions of the IDTs are canceled in R/T of Eq. (3) but also the factors responsible for the propagation phase and attenuation on free surface disappear.

It can be easily shown (see below) that for a weak ideal reflector ($\kappa \to 0$), in a lossless case, the ratio $|\mathrm{R/T}|$ exhibits a $\sin(x)/x$-type behaviour as a function of frequency with numerous minima, or zeros, on both sides of the main lobe. The presence of attenuation adjusts these minima into notches of finite level. A high level of attenuation results in the smoothening of the notches and, for a long structure, the notches may completely disappear. In this paper, we show that measuring the depth of the notches of $|\mathrm{R/T}|$ provides a direct method for determining the attenuation in periodic reflecting gratings.

III. Theory

A. Attenuation

According to the notation of Ref. [7], the COM reflection and transmission coefficients for a grating of length L are

$$\mathrm{R} = \frac{i\kappa^* \sin(\Delta \mathrm{L})}{\Delta \cos(\Delta \mathrm{L}) + i\delta \sin(\Delta \mathrm{L})}, \tag{4}$$

$$\mathrm{T} = \frac{\Delta}{\Delta \cos(\Delta \mathrm{L}) + i\delta \sin(\Delta \mathrm{L})}, \tag{5}$$

where

$$\delta = 2\pi \frac{\mathrm{f} - \mathrm{f_c}}{\mathrm{v}} - i\gamma = \delta_0 - i\gamma \tag{6}$$

is the frequency detuning with losses incorporated in γ, and

$$\Delta = \sqrt{\delta^2 - |\kappa|^2}. \tag{7}$$

Here, κ is the reflectivity. The ratio of the reflection and transmission coefficients, according to the COM theory, is obtained dividing Eq. (4) by Eq. (5):

$$\frac{\mathrm{R}}{\mathrm{T}} = i\frac{\kappa^* \sin(\Delta \mathrm{L})}{\Delta}. \tag{8}$$

For the n^{th} zeros around the main lobe ($n \neq 0$),

$$\Delta_n \mathrm{L} = \pm n\pi \Rightarrow \Delta_n = \pm \frac{n\pi}{\mathrm{L}}. \tag{9}$$

Assuming that the attenuation does not appreciably shift the zeros of R/T in frequency, we may omit γ from δ of Eq. (6) and from Δ of Eq. (7) and write for the n^{th} zero at f_n:

$$\begin{aligned} \delta_{0n} &= 2\pi \frac{\mathrm{f}_n - \mathrm{f_c}}{\mathrm{v}}, \\ \Delta_{0n} &= \sqrt{\delta_{0n}^2 - |\kappa|^2} \simeq \pm \frac{n\pi}{\mathrm{L}} \\ \Rightarrow \delta_{0n} &\simeq \sqrt{|\kappa|^2 + \left(\frac{n\pi}{\mathrm{L}}\right)^2}. \end{aligned} \tag{10}$$

In the general case, we have

$$\Delta_n = \sqrt{(\delta_{0n} - i\gamma)^2 - |\kappa|^2} \simeq \Delta_{0n}\sqrt{1 - i\frac{2\delta_{0n}\gamma}{\Delta_{0n}^2}}, \tag{11}$$

where the term $-\gamma^2$ was neglected. This simplification implies the assumption that $\Delta_{0n}^2 = \delta_{0n}^2 - |\kappa|^2 \gg \gamma^2$, *i.e.*, that the attenuation is not too strong. This is justified since the value of Δ is close to zero only in the immediate vicinity of the stopband edges, and the zeros of $|\mathrm{R/T}|$ are farther apart. Further, provided that $\Delta_{0n}^2 \gg \gamma^2$, the complex term under the square root in Eq. (11) is small, and we obtain from the Taylor expansion

$$\Delta_n \simeq \Delta_{0n}\left(1 - i\frac{\delta_{0n}\gamma}{\Delta_{0n}^2}\right) = \Delta_{0n} - i\frac{\delta_{0n}\gamma}{\Delta_{0n}}. \tag{12}$$

Let us now approximate R/T at the notches. Substitution of Eq. (12) into Eq. (8) yields

$$\left.\frac{\mathrm{R}}{\mathrm{T}}\right|_{\mathrm{notch}} \simeq i\frac{\kappa^*}{\Delta_{0n}} \sin\left(\Delta_{0n}\mathrm{L} - i\frac{\delta_{0n}\gamma \mathrm{L}}{\Delta_{0n}}\right), \tag{13}$$

where the (small) complex part of Δ_n was dropped from the denominator. Noting that $\sin(\Delta_{0n}\mathrm{L}) = 0$, Eq. (13) can be further reduced into

$$\left.\frac{\mathrm{R}}{\mathrm{T}}\right|_{\mathrm{notch}} \simeq \frac{\kappa^*}{\Delta_{0n}} \cos(\Delta_{0n}\mathrm{L}) \mathrm{sinh}\left(\frac{\delta_{0n}\gamma \mathrm{L}}{\Delta_{0n}}\right). \tag{14}$$

For the notches, $\Delta_{0n}\mathrm{L} = \pm n\pi$, and thus $\cos(\Delta_{0n}\mathrm{L}) = \pm 1$. Assuming that $\delta_{0n}\gamma \mathrm{L} \ll \Delta_{0n}$, the hyperbolic sine may be approximated by its argument. Then,

$$\left.\frac{\mathrm{R}}{\mathrm{T}}\right|_{\mathrm{notch}} \simeq \pm\frac{\kappa^*\delta_{0n}\gamma \mathrm{L}}{\Delta_{0n}^2} = \pm\frac{\kappa^*\delta_{0n}\gamma \mathrm{L}^3}{n^2\pi^2}, \tag{15}$$

where the latter form, obtained by inserting Δ_{0n} from Eq. (10), indicates that the finite value of R/T at the notches is determined by the attenuation in the gratings. This is the key point in this paper. The values of the magnitude of R/T at the notches are direct measures of the attenuation. Note that for small values of reflectivity κ, $\delta_{0n}/n^2 \sim 1/n$, *i. e.*, the magnitude of R/T at notches is inversely proportional to the notch order n. Moreover, for a real-valued κ, the ratio R/T at the notches becomes real while for the center of the stopband it is purely imaginary. Taking δ_{0n} from Eq. (10), and denoting $\mathrm{f}_n - \mathrm{f_c} = \Delta \mathrm{f}_n$, we find after a few manipulations a form in which the reflectivity is normalized to the wavelength and the attenuation is associated with the grating length:

$$\left.\frac{\mathrm{R}}{\mathrm{T}}\right|_{\mathrm{notch}} \simeq \pm\frac{2}{n^2\pi}\left(\frac{\Delta \mathrm{f}_n}{\mathrm{f_c}}\right)\left(\frac{\mathrm{L}}{\lambda_0}\right)^2 (\kappa^*\lambda_0)\,\gamma \mathrm{L}. \tag{16}$$

For the fundamental mode of operation one wavelength equals the width of two electrode periods, $\lambda_0 = 2p$ and the grating length is $L = (N_{el} - 1)\lambda_0/2$. Then, Eq. (16) may be approximated as

$$\left.\frac{R}{T}\right|_{\text{notch}}^{\text{fundamental}} \simeq \pm\frac{2}{n^2\pi}\left(\frac{\Delta f_n}{f_c}\right)\left(\frac{N_{el}-1}{2}\right)^3(\kappa^*\lambda_0)\,(\gamma\lambda_0), \tag{17}$$

where the normalized form of attenuation $\gamma\lambda_0$ is displayed.

The formula (17) may be interpreted in simple terms for an array of reflecting elements. For weak reflectivity, neglecting multiple reflections, one may estimate the signal reflected from the array of reflecting elements, evaluated at the first notches, from the following elementary consideration. In a Bragg condition, *i. e.*, at the center frequency f_c, all the reflected contributions are in phase and thus sum up. This can be represented as the sum of N parallel vectors of equal magnitude, see Fig. 3. If the reflectivity for a single element is $\kappa\lambda_0/2 = \kappa p$, where $p = \lambda/2$ is the periodicity of the array, the total reflectivity is obtained as $R = N \cdot (\kappa\lambda_0/2) \cdot A = N \cdot (\kappa p) \cdot A$.

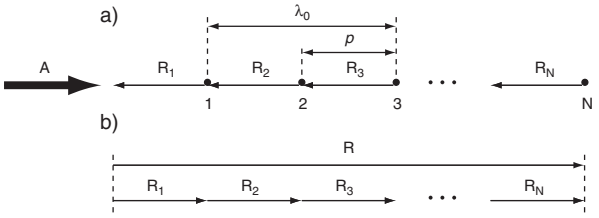

Fig. 3. Schematic of the condition for synchronous reflection in the absence of multiple reflections. a) Setup for reflection. A is the incident signal and the partial reflected signals R_i of equal magnitude sum up in phase to yield the total reflected signal R. $p = \lambda_0/2$ is the period of the array. b) Phase diagram. The reference phase is that of the first reflected contribution.

In the case of operation at frequencies detuned from the center frequency ($f = f_c + \Delta f$), in the simplified model with the multiple reflections ignored, there is a regular phase shift $\Delta\varphi = 2\pi\Delta f/f_c$ between the reflected partial signals. Then the magnitude of the reflection coefficient is smaller than in the synchronous case of Fig. 3. The associated vector sum is illustrated in Fig. 4(a). For a certain detuning value, one arrives at a diagram approximating a circle, where the resultant reflectivity vanishes, see Fig. 4(b). This corresponds to the first notch of the reflection coefficient. The radius r of the circle is

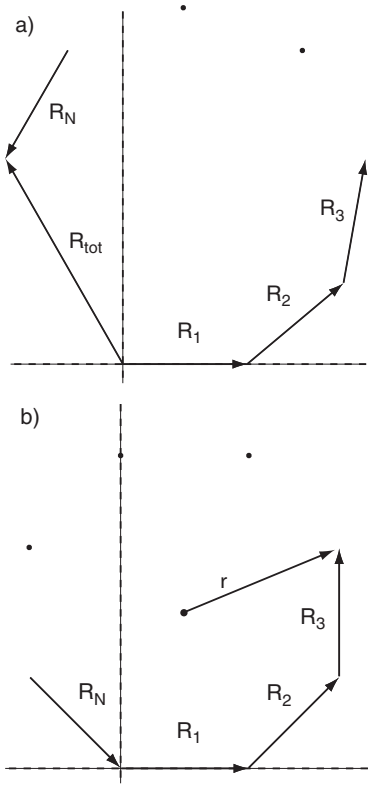

Fig. 4. Vector representation of an asynchronous reflection in the absence of attenuation and multiple reflections. The partial reflected signals R_i of equal magnitude sum up with a regular phase shift. a) General case. b) Circular diagram corresponding to vanishing reflection.

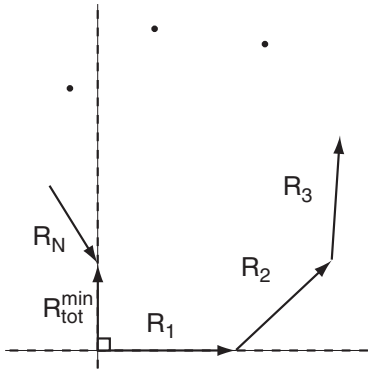

Fig. 5. Vector representation of an asynchronous reflection, with finite attenuation, in the absence of multiple reflections. The partial reflected signals R_i having magnitudes decreasing with index i sum up with a phase shift. Here, the case yielding a minimum value of total reflection coefficient is shown.

roughly equal to the sum of the magnitudes of the reflection contributions divided by 2π.

If a finite attenuation is present, the magnitude of the contributions of reflectivity R_i gradually de-

creases. Consequently, the radius r in Fig. 4(b) is no longer constant but also decreases and the zero of reflection coefficient is transformed into a minimum value, see Fig. 5. On comparison of Figs. 3 and 5, it is evident that the minimum of the reflected signal is in phase quadrature (shift of 90°) with respect to the synchronous reflection.

The minimum amplitude of $\mathrm{R_{tot}}$ at the first notch can be estimated. Let us approximate the decrease of amplitude for the last reflected contribution $\mathrm{R_N}$ as

$$\Delta \mathrm{R_N} = \kappa p \mathrm{A} - \kappa p \mathrm{A} e^{-2\gamma p \mathrm{N}} \approx (\kappa p)(\gamma \lambda_0 \mathrm{N})\mathrm{A}, \quad (18)$$

where a low total attenuation is assumed and $\gamma\lambda_0$ is expressed in nepers per wavelength. The factor 2 originates from the propagation of the incident wave through the grating, $\mathrm{L} = \mathrm{N}p$, and the propagation of the contribution reflected from the $\mathrm{N^{th}}$ element of the array ($\mathrm{R_N}$). Then, the average decrease of amplitude for the reflected signals is $(\kappa p)(\gamma\lambda_0\mathrm{N})/2{\cdot}\mathrm{A} = (\kappa p)(\gamma p)\,\mathrm{N}\cdot\mathrm{A}$. The total decrease in the sum of the magnitudes of the N reflected contributions is thus $\mathrm{N}\cdot(\kappa p)(\gamma p)\,\mathrm{N}\cdot\mathrm{A} = (\kappa p)(\gamma p)\,\mathrm{N}^2\cdot\mathrm{A}$. To obtain the corresponding decrease in the length of the radius, the decrease in the sum of the magnitudes of the reflected contributions can be evaluated from two semicircles with radii $\mathrm{r_1}$ and $\mathrm{r_{final}}$, resulting in the approximation

$$\mathrm{r_1} - \mathrm{r_{final}} \approx \frac{(\kappa p)(\gamma p)\,\mathrm{N}^2}{2\pi}\mathrm{A}, \quad (19)$$

which roughly corresponds to half of the minimum of the reflected amplitude $\mathrm{R_{tot}^{min}}$. Along with this reasoning, the estimated first minimum of the reflection coefficient is

$$\frac{\mathrm{R_{tot}^{min}}}{\mathrm{A}} \approx 2 \cdot \frac{(\kappa p)(\gamma p)\,\mathrm{N}^2}{2\pi} = \frac{\mathrm{N}^2}{4\pi}\,(\gamma\lambda_0)\,(\kappa\lambda_0). \quad (20)$$

Comparing Eq. (20) to Eq. (17) with $n = 1$, it is evident that the two results given by the two different approaches closely resemble each other, in particular, if one takes into account that in the region of the first notch,

$$\left(\frac{\Delta \mathrm{f_1}}{\mathrm{f_c}}\right)\mathrm{N_{el}} \simeq 1. \quad (21)$$

From Eq. (17), an estimate for $\gamma\lambda_0$ is obtained:

$$\gamma\lambda_0 = \frac{4n^2\pi\left(\left|\frac{\mathrm{R}}{\mathrm{T}}\right|_{\mathrm{notch}}^{\mathrm{fundamental}}\right)}{\left|\frac{\Delta \mathrm{f}_n}{\mathrm{f_c}}\right|(\mathrm{N_{el}}-1)^3\,|\kappa\lambda_0|}, \quad (22)$$

where $|\Delta \mathrm{f}_n/\mathrm{f_c}|$ is the deviation from the center frequency of the grating, defined by the frequencies $\mathrm{f}^n_{1,\mathrm{gr}}$ and $\mathrm{f}^n_{2,\mathrm{gr}}$ corresponding to the n^{th} notches of $|\mathrm{R/T}|$

$$\frac{\Delta \mathrm{f}_n}{\mathrm{f_c}} = \frac{\mathrm{f}^n_{2,\mathrm{gr}} - \mathrm{f}^n_{1,\mathrm{gr}}}{\mathrm{f}^n_{1,\mathrm{gr}} + \mathrm{f}^n_{2,\mathrm{gr}}}. \quad (23)$$

According to the COM model, the notches in the magnitude of the reflection coefficient are found at

$$\begin{aligned}\frac{\Delta \mathrm{f}_n}{\mathrm{f_c}} &= \sqrt{\left(\frac{|\kappa\lambda_0|}{2\pi}\right)^2 + \left(\frac{n\lambda_0}{2\mathrm{L}}\right)^2} \\ &= \sqrt{\left(\frac{|\kappa\lambda_0|}{2\pi}\right)^2 + \left(\frac{n}{\mathrm{N_{el}}-1}\right)^2},\end{aligned} \quad (24)$$

and the reflectivity $|\kappa\lambda_0|$ may be substituted in Eq. (22) to yield

$$\gamma\lambda_0 = \frac{2\left(\left|\frac{\mathrm{R}}{\mathrm{T}}\right|_{\mathrm{notch}}^{\mathrm{fundamental}}\right)}{\left|\frac{\Delta \mathrm{f}_n}{\mathrm{f_c}}\right|(\mathrm{N_{el}}-1)^3\sqrt{\left(\frac{\Delta \mathrm{f}_n}{\mathrm{f_c}}\right)^2 - \left(\frac{n}{\mathrm{N_{el}}-1}\right)^2}}. \quad (25)$$

The physical interpretation of Eq. (24) is that multiple reflections render the grating effectively shorter. For very long gratings, the waves do not penetrate to the ends of the grating at the stopband frequencies. Then, the effect of the grating length is negligible. For short gratings, the term with L^2 in the denominator is the dominating term in Eq. (24). The coupling-of-modes (COM) model is derived for counterpropagating waves in a periodic system of perturbations. Thus, the accuracy of the model in the case of a short reflector with pronounced end effects is reduced. The extraction of $|\kappa\lambda_0|$ from Eq. (24) implies obtaining a small value via the subtraction of two relatively large values, which is disadvantageous for the accuracy. It is evident that Eq. (24) is accurate only if the term $(\lambda_0/2\mathrm{L})^2$ is small. In this paper, alternative methods are applied for the extraction of the reflectivity, and Eq. (22) is used to evaluate the attenuation parameter.

According to Eq. (17) the depth of the notches of $|\mathrm{R/T}|$ increases with the deviation from the center frequency. Since the relative deviation from $\mathrm{f_c}$ at the notches, $\Delta \mathrm{f}_n/\mathrm{f_c}$, is roughly proportional to the notch order n, the level of $|\mathrm{R/T}|$ at the notches should be inversely proportional to n. This can be verified simply by following the guidelines of the elementary estimation. The vector representation for asynchronous reflection in Fig. 5 is illustrated for a

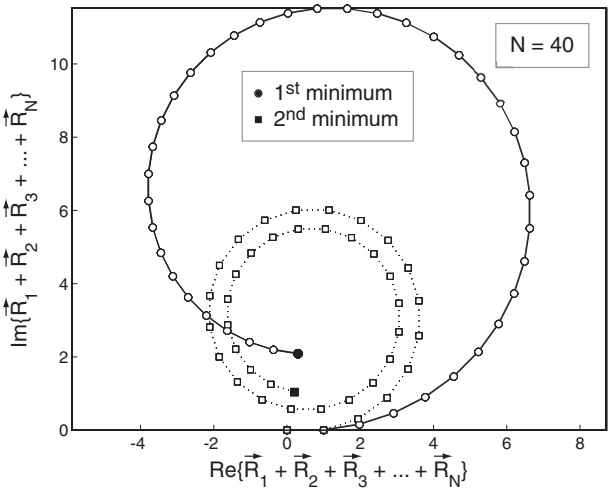

Fig. 6. Schematic of the total reflection amplitude R at the first minima of the reflection response obtained as a vector sum for the asynchronous lossy condition. The circles (○) and squares (□) indicate the cumulative vector sum for the first and second notches of the reflection response. Attempts to reduce R to the absolute minimum were not made.

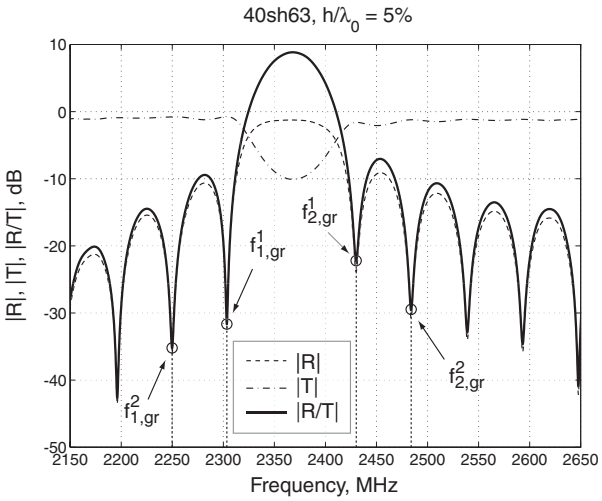

Fig. 7. Magnitudes of the reflection and transmission coefficients (|R|, |T|) and their ratio (|R/T|) as a function of frequency for a finite grating. The first ($f^1_{1,gr}$ and $f^1_{2,gr}$) and second ($f^2_{1,gr}$ and $f^2_{2,gr}$) notches of |R/T| are shown. Here, the grating has 40 short-circuited electrodes with $a/p = 0.63$.

reflecting array with 40 elements in Fig. 6. The vector sums simulating the total complex reflectivity at the first two minima of the reflection coefficient in the absence of multiple reflections are shown. Attempts to reduce R to the absolute minimum were not pursued. However, it is clearly seen that the level of the reflection coefficient at the notches decreases with the notch order n.

This feature is also observed in the measured |R/T| response, illustrated in Fig. 7. In the particular case presented here, the first upper notch ($f^1_{gr,2}$) is evidently at a higher level than the lower first notch ($f^1_{gr,1}$). The reason for this feature is likely to be the scattering of the Rayleigh SAW into the bulk—in the form of a slow shear bulk wave (SSBAW)—which begins within the grating on 128° $LiNbO_3$ at frequencies in the region of the first upper notch of |R/T|.

Here, the normalized attenuation values are obtained from the first lower notch of the ratio |R/T|.

B. Reflectivity

For the center frequency, the detuning δ_0 in Eq. (6) equals zero. Estimates for the normalized reflectivity can be extracted from the center-frequency values of the magnitudes of the reflection and transmission coefficients, or from the ratio |R/T|. For simple expressions, one may evaluate the lossless case ($\gamma = 0$ in Eq. (6)) from Eqs. (4), (5) and (8):

$$|\kappa\lambda_0|_{\mathrm{R}} = \frac{\lambda_0}{\mathrm{L}}\mathrm{atanh}(|\mathrm{R}(\mathrm{f_c})|), \tag{26}$$

$$|\kappa\lambda_0|_{\mathrm{T}} = \frac{\lambda_0}{\mathrm{L}}\mathrm{acosh}\left(\frac{1}{|\mathrm{T}(\mathrm{f_c})|}\right), \tag{27}$$

$$|\kappa\lambda_0|_{\mathrm{R/T}} = \frac{\lambda_0}{\mathrm{L}}\mathrm{asinh}\left(\left|\frac{\mathrm{R}(\mathrm{f_c})}{\mathrm{T}(\mathrm{f_c})}\right|\right). \tag{28}$$

However, nonzero attenuation affects the accuracy of the results. Inclusion of γ in Eq. (6) leads to the expressions

$$\mathrm{R}(\mathrm{f_c}) = \frac{i\kappa^* \sinh(\Delta_c \mathrm{L})}{\Delta_c \cosh(\Delta_c \mathrm{L}) + \gamma \sinh(\Delta_c \mathrm{L})}, \tag{29}$$

$$\mathrm{T}(\mathrm{f_c}) = \frac{\Delta_c}{\Delta_c \cosh(\Delta_c \mathrm{L}) + \gamma \sinh(\Delta_c \mathrm{L})}, \tag{30}$$

$$\frac{\mathrm{R}(\mathrm{f_c})}{\mathrm{T}(\mathrm{f_c})} = \frac{i\kappa^* \sinh(\Delta_c \mathrm{L})}{\Delta_c}, \tag{31}$$

$$\text{where } \Delta_c = \sqrt{\gamma^2 + |\kappa|^2}. \tag{32}$$

Since we have an estimate for the loss normalized to the input power observed in the measurements,

$$\mathrm{Loss} = 1 - |\mathrm{R}|^2 - |\mathrm{T}|^2 = 1 - e^{-2\gamma \mathrm{L}}, \tag{33}$$

we can evaluate $\gamma(\mathrm{f_c})$:

$$\gamma(\mathrm{f_c}) = -\frac{\log_e(|\mathrm{R}(\mathrm{f_c})|^2 + |\mathrm{T}(\mathrm{f_c})|^2)}{2\mathrm{L}}, \tag{34}$$

where |R| and |T| are obtained from Eq. (2). Knowing the attenuation at the center frequency, $\gamma(\mathrm{f_c})$,

we can estimate the reflectivity iteratively from any of Eqs. (29)–(31). For the iteration, we use the Newton method:

$$\kappa_{n+1} = \kappa_n - \frac{f(\kappa_n)}{f'(\kappa_n)}, \tag{35}$$

where $f(\kappa) = 0$ is any of the functions Eqs. (29)–(31) with all terms on left-hand side, and $f'(\kappa)$ is its derivative. The initial value used is $|\kappa\lambda_0|$ taken from Eqs. (26)–(28), respectively.

A comparison of the lossless and lossy cases is shown in Fig. 8, where $|R(f_c)|$, $|T(f_c)|$ and $|R(f_c)/T(f_c)|$ are shown as a function of $|\kappa\lambda_0|$. The curves for the lossless cases are obtained from Eqs. (4), (5) and (8), and those for the lossy cases from Eqs. (29)–(31), having $|\kappa\lambda_0|$ as a variable. The center-frequency attenuation, obtained from Eq. (34) and used as a parameter in Eqs. (29)–(31), is extracted from the measured response of a test structure having an open-circuited 20-electrode grating with $a/p = 0.53$. The illustration indicates that the smallest relative change in the reflectivity due to the inclusion of the losses is obtained for $|R(f_c)/T(f_c)|$. For $|R(f_c)|$ and $|T(f_c)|$, the discrepancy is large. For the latter, the deviation appears particularly pronounced for low values of reflectivity. The effect observed in Fig. 8 is a consequence of the fact that attenuation always decreases the signal level. The magnitude of the reflection coefficient, obtained from the measured frequency response, is reduced due to the attenuation. Thus, the reflectivity evaluated using Eq. (26) is underestimated. Similarily, the magnitude of the measured transmission coefficient is lowered by the presence of attenuation, which implies an overestimation of the reflectivity in Eq. (27). As for the ratio of the reflection and transmission coefficients, Eq. (28), the effect of the attenuation is to a large extent canceled since the reference measurement—with grating losses absent—is not needed. The reflected and transmitted waves propagate a comparable distance inside the grating, compensating for a significant part of the attenuation.

Furthermore, in both the lossy and lossless curves of $|R(f_c)|$ and $|T(f_c)|$, there are areas where the slopes are close to zero. Consequently, small changes in the values of the reflection or transmission coefficients result in large shifts in the reflectivity values obtained. This property also complicates the convergence of the iteration procedure. Our consideration agrees to that of Ref. [6]: the ratio of the reflection and transmission coefficients is the most accurate method for determining the reflectivity of a grating.

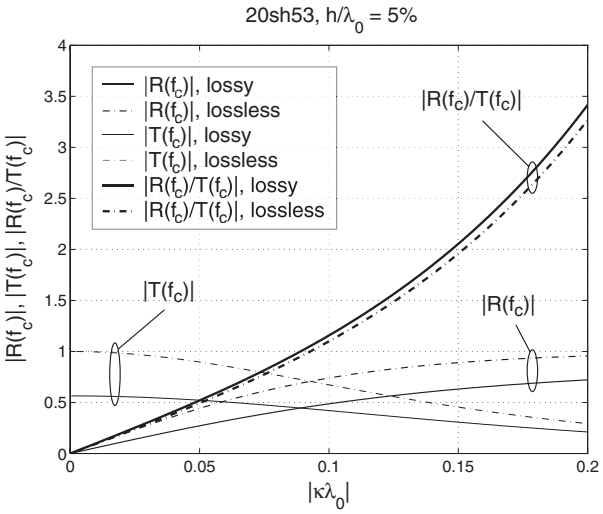

Fig. 8. Depencences of $|R(f_c)|$, $|T(f_c)|$ and $|R(f_c)|/|T(f_c)|$ on $|\kappa\lambda_0|$ for the lossy and lossless cases.

Due to the attenuation incorporated in the measurement results, Eqs. (4), (5) and (8)—as well as the Newton iteration applied to Eqs. (29)–(31)—produce different values for $|\kappa\lambda_0|$. For a weak total reflectivity of the grating, the energy scattered from the grating into the bulk may be comparable to or even larger than the energy reflected. In such a case, the relative decrease induced in the reflection coefficient, equal to 50% or more of the lossless value, leads to a serious underestimation of the normalized reflectivity. This is manifested in all the methods for extracting $|\kappa\lambda_0|$ which employ the reflected signal $S_{11,\,gr}^{\text{time-gated}}$, Eqs. (4), (8), (29) and (31). Examples of extracted values of reflectivity are shown in Fig. 9.

IV. Results

The method proposed for directly evaluating the attenuation was applied to the ratio R/T obtained from measured S parameter data. The parameter $\gamma\lambda_0$ estimated from Eq. (22) at the first lower notch of |R/T| is presented in Fig. 10. The results for a grating with 20 floating electrodes and for a 40-electrode short-circuited grating are shown for selected aluminium thicknesses h/λ and metallisation ratios a/p. For the purpose of comparison, values obtained for 3-electrode open- and short-circuited gratings through simulations [4] are also shown. The values extracted from experimental data are indicated by solid lines and markers with black face, while the reference values obtained from simulations of short reflectors are plotted with dash-dotted lines

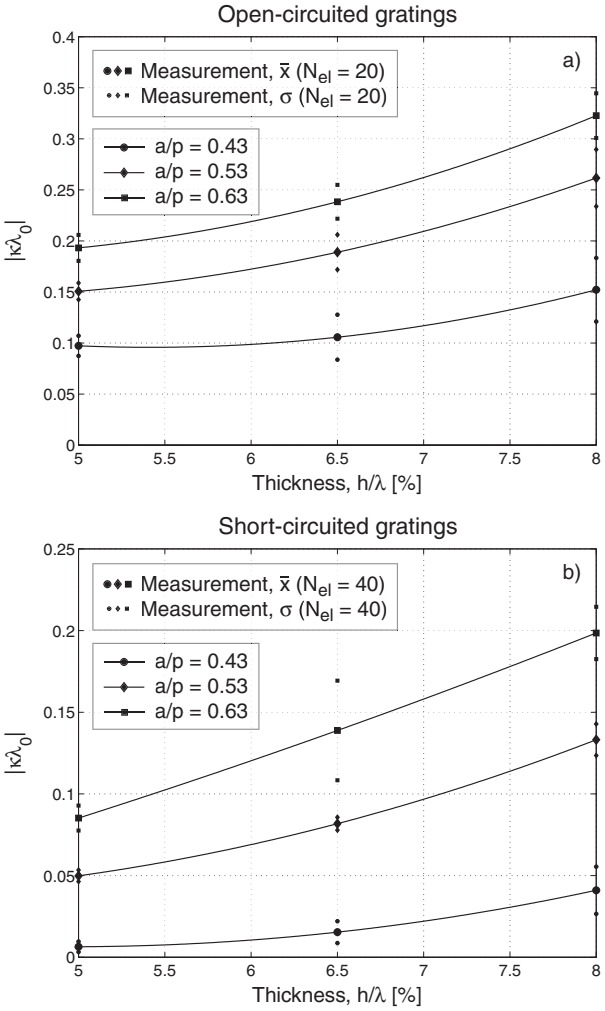

Fig. 9. Reflectivity ($\bar{x} \pm \sigma$) of a grating extracted by applying the Newton iteration of Eq. (35) to the center-frequency value of measured |R/T|, Eq. (31). The average values are denoted with solid lines and large markers while the error bounds are indicated by small markers. (a) Grating with 20 floating electrodes. (b) 40-electrode short-circuited grating.

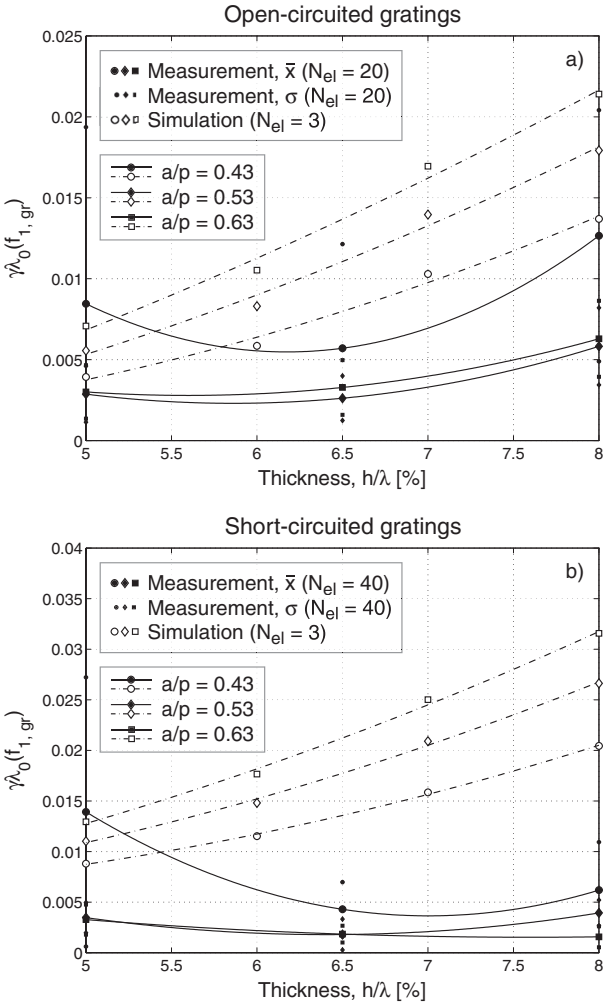

Fig. 10. Attenuation ($\bar{x} \pm \sigma$) inside a grating extracted according to Eq. (22) from the first lower notch ($f_{gr,1}$) of |R/T| of the measured responses. The average values are denoted with solid lines and large markers with black face. The error bounds are indicated by small markers with black face. For comparison, the attenuation evaluated for short gratings ($N_{el} = 3$), obtained through simulations [4], is also shown (dash-dotted lines, markers with white face). (a) Grating with 20 floating electrodes. (b) 40-electrode short-circuited grating.

and markers with white face. Every experimental point is a statistical average of several measurements.

The magnitude of the normalized attenuation for the 20- and 40-electrode gratings is lower than that obtained for short gratings. This is expected since, for fundamental-mode reflectors, an infinite periodic grating exhibits no synchronous scattering into the bulk at the Bragg frequency. The attenuation due to the scattering from the ends of the grating is probably canceled when R/T is considered. On the contrary, for a short structure, the periodicity has a weak influence and the end effects are emphasized. The attenuation extracted from the measured responses does not exhibit a behaviour similar to that in short reflectors as functions of h/λ_0 or a/p. It is likely that in some cases, *e. g.*, for a short-circuited grating having $a/p = 0.43$, the reflectivity is underestimated, see Sec. III-B. The normalized attenuation obtained by Eq. (22) would then be overestimated. The high values of attenuation obtained for open-circuited gratings with $a/p = 0.43$ can not be explained by an underestimated value of the reflectivity, though. It is evident from Fig. 10(a) that the said data points are are subject to considerable

statistical variation. A likely explanation for the result lies in the inaccuracies in the electrical measurements, not originally carried out in view of the requirements of high precision of the new characterization technique proposed in this work.

The purpose of the present paper is to demonstrate a method for the extraction of the attenuation parameter $\gamma\lambda_0$. Further investigations on optimizing the test structure geometry and careful measurements are necessary for effective application of the method described.

V. Discussion

We have shown that an investigation of the ratio of the reflection and transmission coefficients of a grating, R/T, yields valuable information about the attenuation of SAW in the grating. In particular, the levels of the notches are determined by γ. Both an elementary estimation and the COM model show that, in the presence of weak attenuation, the notches are transformed from zeros of the reflection coefficient into sharp minima with a signal level proportional to the attenuation parameter and phase orthogonal to that of the center of the stopband. This relation allows, for the first time, to directly measure the attenuation in a grating. First examples for such measurements given for 128° $LiNbO_3$ at 2.5 GHz indicate that careful control of the fabrication and high-precision measurements are needed for the application of the proposed technique. The investigation of the ratio R/T also allows one to extract the reflectivity of a grating with a better accuracy than that obtained using the reflection or transmission coefficients separately.

Acknowledgments

The authors are grateful to Paul Brown for carrying out the electrical measurements. The first author further acknowledges Helsinki University of Technology and the Foundation of Technology (Finland) for scholarships.

References

[1] P. V. Wright, "A New Generalized Modeling of SAW Transducers and Gratings," *Proc. 1989 IEEE Freq. Contr. Symp.*, pp. 596–605.

[2] C. S. Hartmann and V. P. Plessky, "Experimental Measurements of Propagation, Attenuation, Reflection, and Scattering of Leaky Waves in Al Electrode Gratings on 41°, 52° and 64°–$LiNbO_3$," *Proc. 1993 IEEE Ultrasonics Symp.*, pp. 1247–1250.

[3] S. Lehtonen, V. P. Plessky, and M. M. Salomaa, "Second-Harmonic Reflectors on 128° $LiNbO_3$," *IEEE Trans. Ultrason., Ferroelectr., Freq. Contr.*, Vol. 50, No. 8, August 2003, pp. 972–978.

[4] S. Lehtonen, V. P. Plessky, and M. M. Salomaa, "Short reflectors operating at the fundamental and second harmonics on 128° $LiNbO_3$," *IEEE Trans. Ultrason., Ferroelectr., Freq. Contr.*, Vol. 51, No. 3, March 2004, pp. 343–351.

[5] P. Wright, "Modeling and experimental measurements of the reflection properties of SAW metallic gratings", *Proc. 1984 IEEE Ultrasonics Symp.*, pp. 54–63.

[6] C. S. Hartmann and B. P. Abbott, "Experimentally Determining the Transduction Magnitude and Phase and the Reflection Magnitude and Phase of SAW SPUDT Structures," *Proc. 1990 IEEE Ultrasonics Symp.*, pp. 37–42.

[7] V. P. Plessky and J. Koskela, "Coupling-of-modes Analysis of SAW Devices," pp. 1–82 in C. C. W. Ruppel and T. Fjeldly, *Advances in Surface Acoustic Wave Technology, Systems and Applications, Vol. 2*, World Scientific, 2001.